A Modular and Cost-Effective Superconducting Generator Design for Offshore Wind Turbines

†

Ozan Keysan, Markus Mueller

Institute for Energy Systems, University of Edinburgh, EH93JL, UK

E-mail: o.keysan@ed.ac.uk

Abstract. For offshore wind energy, there is a trend towards larger wind turbines. Larger wind turbines mean The increased tower head mass and therefore increased installation cost. Superconducting generators have the potential to reduce the tower head mass for large offshore wind turbines. However, a HTS generator should be as reliable as conventional generators for a successful entry to the market. In this study, machine design with a stationary superconducting dc-field winding is proposed which increases the reliability. A 10 MW 10 rpm

devami yazilacak

S4E Superconducting wind turbine generators are proposed to reduce the tower-head mass for very large (¿10 MW) wind turbines. This will help to reduce the manufacturing and installation cost. Most of the proposed designs use the superconducting synchronous generator concept, which consists of a rotating superconducting field winding and copper- based armature winding. However, the authors think this topology is not designed according to the requirements of offshore conditions. Firstly, offshore wind turbine generators operate in harsh conditions and are exposed significant vibration levels in the nacelle. Secondly, maintenance of offshore wind turbines are expensive and any failures result in long down periods adding lost generation income on top of the repair cost. A superconducting wind turbine should satisfy the following requirements to compete with the existing power take-off technologies: - High reliability (including subsystems such as the refrigeration system) to minimise operation and maintenance costs. - Redundancy in generator systems to minimise down time. - Modularity to enable on-site repairs without requiring large offshore cranes. - Competitive cost compared to alternative power take-off systems such as direct-drive permanent magnet generators and geared systems. A novel superconducting machine concept has been proposed by the authors in [1], the novelty of the design lays in having a single loop-shaped stationary superconducting field winding. This configuration eliminates the rotating transfer coupler, which is the single point of failure for most of the existing designs. Furthermore, there is no electromagnetic torque acting on the superconducting coil, which simplifies the design of the rotor structure. The rotor just consists of modular iron-cored claw poles, which can be installed or removed in situ. An improved version of the claw-pole topology will be presented in this paper, which has two independent armature windings further increasing the modularity. Furthermore, the field winding can be manufactured using three or four independent cryostats, all of which can be replaced without disassembling whole machine. The final advantage of the proposed design is the minimal use of

†Supported by MARINA

superconducting coil, which makes the design economically competitive to conventional power take-off systems. For example, a 10 MW, 10 rpm machine is designed, the machine uses 15 km of MgB2 wire at 20 K. The outer diameter of the machine is 6.5 m and weighs 184 tonnes including the structural mass.

1. Introduction

The average size of the offshore wind turbines are continuously increasing. It was 2 MW a decade ago, but now increased to 5 MW [?]. The installation and maintenance cost of large offshore wind turbines are cheaper per MW compared to smaller wind turbines, and it takes less time to build a wind farm with larger turbines, which all help to reduce the cost of energy [?]. It is aimed to build 10 MW, and even 20 MW, wind turbines [?]. However, the tower head mass of larger wind turbines becomes a critical issue, which is estimated as 760 t for a 10 MW turbine [?].

Direct-drive superconducting machines are proposed to minimize the tower head-mass and increase the energy yield [?, ?, ?]. It is stated in [?] that a 6 MW HTS direct drive generator may have 50 % of the mass of a direct drive PM generator and the lower mass of generator may enable transport and installation of the turbine in one piece.

Data from direct-drive systems have been collected to compare mass to torque ratio of HTS machines with other type of generators and the result is presented in a bubble chart in Fig. 1 and tabulated in Table 1. Although, some designs are just conceptual designs and some are commercial products, the graph provides a good understanding of torque density capability of HTS machines. The dashed line represents ratio of generator mass to torque for permanent-magnet machines which is estimated as 25 kg/kNm by Bang *et al.* in [?]. The continuous line represents the linear trend line estimated using the HTS machines in the graph. The equation of the trend line can be represented as:

$$Mass(t) = 0.011 \times Torque(kNm) + 45 \tag{1}$$

From the graph, it is clear that HTS machines are lighter than PM generators for applications with torque requirements larger than 3000 kNm. Although, superconducting machines are lighter than conventional generators (e.g. geared doubly-fed induction generators or direct-drive permanent magnet generators), low-mass is not the only desired property for offshore wind turbines. Reliability and serviceability is also very important for offshore wind turbines, as any unexpected maintenance is very time consuming and expensive. Furthermore, any down-time related to generator faults add lost energy generation income on top of the repair cost. Therefore, in order to penetrate into the offshore renewable energy market, the superconducting generators should be as reliable and easy to maintain as the conventional generators.

Compared to conventional generators superconducting generators have the disadvantage of having extra subsystems such as cryocooler, vacuum system etc. In this paper, a novel superconducting generator topology that is reliable and modular will be presented.

!! Refleri ekle Offshore wind turbine applications have challenging requirements. Repair and maintenance in offshore wind turbines are time consuming and expensive. Thus, the superconducting generator should be as reliable as the conventional generator systems. Furthermore, any critical system should have redundancy to get fail-safe operation. It is desirable to have modularity in the power take-off system to make transportation, installation and maintenance easier.

Table 1: Torque density comparison conventional and superconducting generators.

	Manufacturer	Power (MW)	Speed (rpm)	Mass (t)	Torque (kNm)	Mass/T (kg/kNm)	Type
1	Harakosan [?]	1.5	18	47.2	796	59.3	PMG
2	The Switch [?]	3.8	21	81	1728	46.9	PMG
3	NewGen [?]	4	19	36.4	2010	18.1	PMG
4	NREL-AMSC [?]	3.1	12.5	90	2368	38.0	PMG†
5	Bang et. al. [?]	5	12	90.8	3979	22.8	TFPM
6		5	12	60.5	3979	15.2	TFPM†
7	NTNU Reference [?]	10	13	260	7346	35.4	PMG
8	NREL-AMSC [?]	6	12.3	177	4658	38.0	PMG†
9		10	11.5	315	8304	37.9	PMG†
10	Bang et. al. [?]	10	10	325	9549	34.0	PMG †
11	Enercon-E126	7.5	12	220	6031	36.4	EESM
12	Lee et. al. [?]	5	230	44	208	212.0	HTSG†
13		5	230	18	208	86.7	HTSG†
14	Maki [?]	2	21.5	54	888	60.8	HTSG
15	NREL-AMSC [?]	3.1	12.5	76	2368	32.1	HTSG
16	AMSC [?]	36.5	120	75	2905	25.8	HTSG
17	Maki [?]	5	14.8	108	3226	33.5	HTSG
18	NREL-AMSC [?]	6	12.3	97	4658	20.8	HTSG
19	Maki [?]	8	12	154	6366	24.2	HTSG
20	Converteam [?]	8	12	100	6366	15.7	HTSG
21	NREL-AMSC [?]	10	11.5	160	8303	19.3	HTSG
22	AMSC [?]	10	11	150	8681	17.3	HTSG
23	Abrahamsen et. al. [?]	10	10.4	88	9182	9.6	HTSG †
24	General Electric [?]	10	10	143	9549	15.0	HTSG †
25	AML [?]	10	10	70	9549	7.3	HTSG †
26	Sung et. al. [?]	10	10	147	9549	15.4	HTSG †
27		10	10	196	9549	20.5	HTSG †

†The machine is not optimised for minimum mass.
†Ring-shaped TFPM.
†The machine is not optimised for minimum mass.
†The diameter is limited to 4.3 m.
†Estimated mass.
†Homopolar superconducting machine.
†Air-cored superconducting synchronous machine.
†The machine is found to be economically infeasible.
†The generator actually uses NbTi low temperature superconductor wire.
†Fully superconducting generator with MgB2 wires.
†With YBCO wire.
†With Bi-2223 wire.

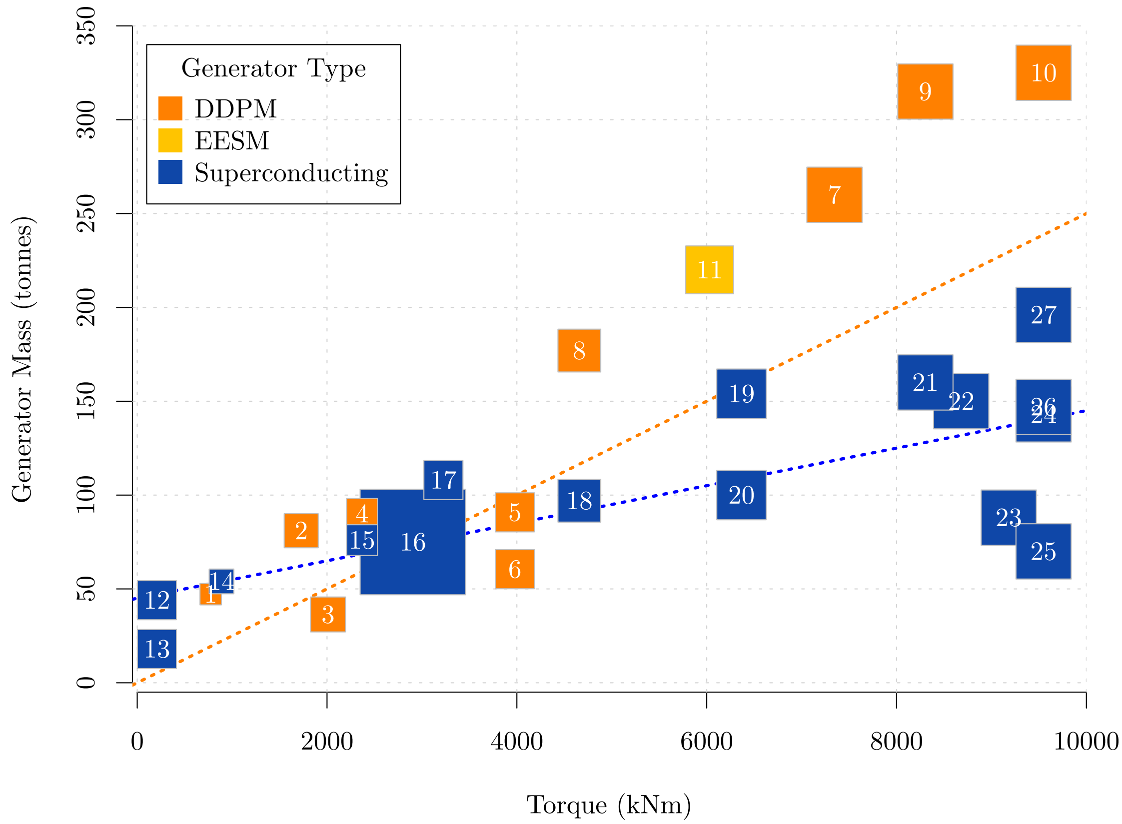

Figure 1: Mass of different large direct-drive machines as a function of the torque, area of the square represents the power rating. DDPM: Direct drive permanent magnet generator, EESM: Electrically excited synchronous machine, Superconducting: High-temperature superconducting generator. Orange line represents generator mass to torque ratio (m/T) of 25 kg/kNm for permanent-magnet machines as given in [?]. Blue line is the linear trend line for the superconducting machines.

Although, the most common superconducting machine topology is the synchronous superconducting machine [?, ?], which has a copper armature winding and a rotating DC-excited superconducting field winding, it may not be the most suitable topology for an offshore wind turbine application. The synchronous generator with a superconducting rotor has the following problems and challenges:

- **Rotating Transfer Coupler:** In a rotating superconducting coil configuration, rotating transfer coupler introduces reliability issues and requires regular maintenance. Furthermore, it is the single point of failure for the whole generator system. It is similar for the electric excitation system.
- **Torque Transfer Structure:** Machines with rotating field superconducting winding require a torque transfer structure that is thermally insulating and structurally sound, which is difficult to design and expensive to manufacture.
- **Transient forces in the SC coil:** Second generation HTS tapes are prone to high stresses and bending. They are exposed to centrifugal and other transient forces in

a rotating superconducting winding design.

- **SC Tape Usage**: In a conventional synchronous superconducting machine, the magnetic flux has to cross the air-gap, vacuum and insulation layers. Thus, the equivalent magnetic gap is larger than the mechanical gap, which increases the superconducting coil requirement.

There are novel machine designs in literature aim to overcome some of these problems. AMSC plans to put the cold heads in the rotor for their 10 MW, 10 rpm generator design [**?**], but the design still requires cryocouplers. General Electric eliminated cryocouplers using a stationary superconducting coil and a rotating copper armature configuration [**?**]. In [**?**], a superconducting generator with stationary superconducting armature and field windings are shown, the machine is similar to a switched reluctance machine.

2. Double Sided Claw Pole Concept

In [**?**] a radial flux claw pole machine is presented. The novelty of the design lays in having a single stationary superconducting field winding, which simplifies the cooling system. The rotor just consists of modular claw poles, which can be easily disassembled if required. That radial flux claw pole machine is improved in this paper as shown in Figure 2. The machine has now two independent armature windings, and claw pole rotor.

The advantages of the double-sided claw pole topology compared to other superconducting machine designs can be listed as:

- The machine has a stationary superconducting field winding, which means: no cryocoupler, no brushes or brushless exciters, no vibrational or rotational forces acting on the SC coil.
- The magnetic attraction forces on the rotor structure are symmetrical and cancel each other, which means reduced structural mass.
- The machine has two armature windings that can be operated independently. Thus, the modularity is increased.
- The machine uses significantly less superconducting coil due to iron-cored structure and loop-shaped field winding.

The 3D FEA model and the flux density vectors in the machine is presented in Figure 3. The flux density vectors shown in Figure 3c verify the operation of the proposed topology, as the magnetic flux created by the superconducting coil links both armature cores through the claw poles as depicted in Figure 2d.

2.1. Material Selection

The proposed design is iron-cored. Thus, the power density of the machine is limited by magnetic saturation, which makes the material selection very critical. Vacuumschmelze

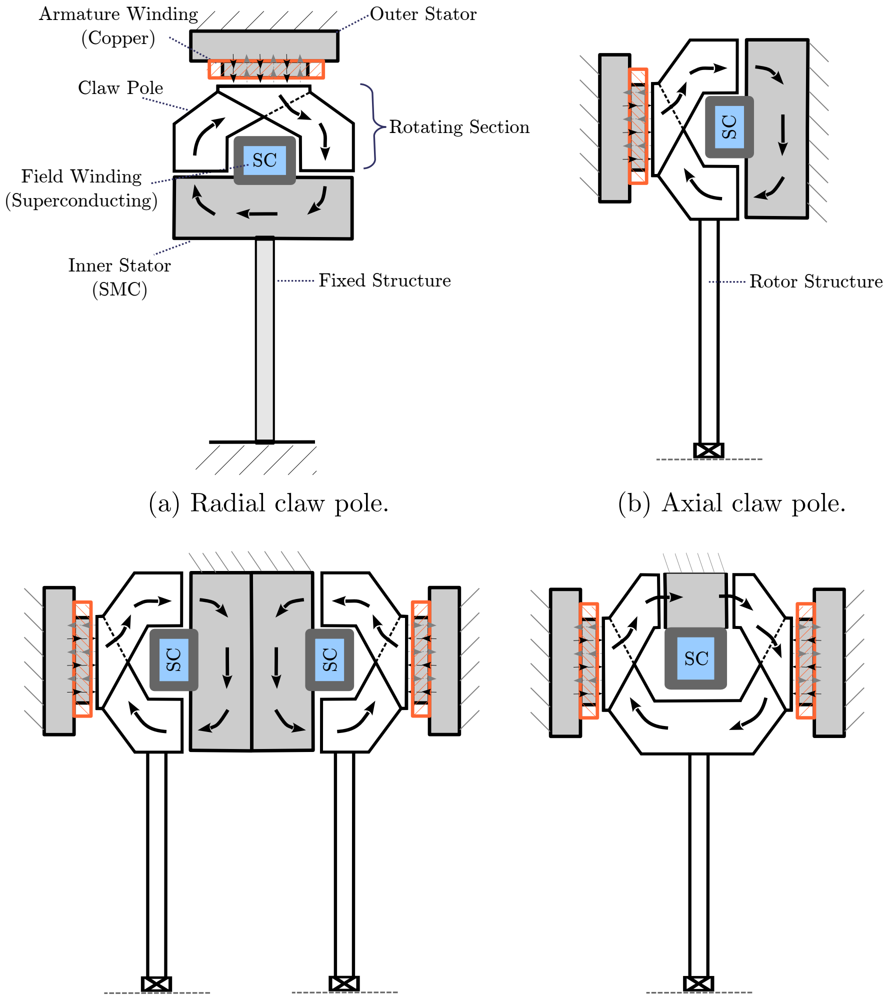

(a) Radial claw pole. (b) Axial claw pole.

(c) Combined axial claw pole. (d) Double-sided claw pole.

Figure 2: Evolution of the claw pole topology.

introduced a cobalt-iron alloy called VacoFlux50, which can be manufactured in laminations and has an impressive magnetic saturation limit with 2.35 T at 16 kA/m [?]. This material is promising for superconducting machine designs with its high saturation limit.

2.2. Sectioned Cryostat

Although, the initial design has a single loop-shaped superconducting field winding, it is difficult to manufacture and install the field winding in one piece in multi-MW scale. In the original design, the cryostat is fixed to the inner surface of the field core as shown in Figure 4a, however, it is also possible to mount another coil on the outer surface of the field core as in Figure 4b. Then, the cryostat can be divided into smaller sections as shown in Figure 4c. This configuration has two main advantages. Firstly, it is easier to manufacture and install the sectioned cryostat compared to full span cryostat. Secondly, two independent cryostat introduces modularity to the system, thus even one

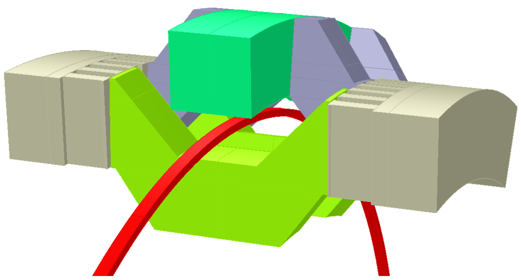

(a) Section of the machine.

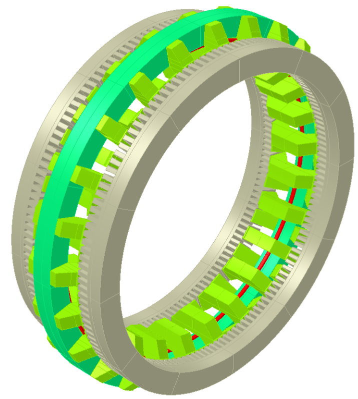

(b) Full machine.

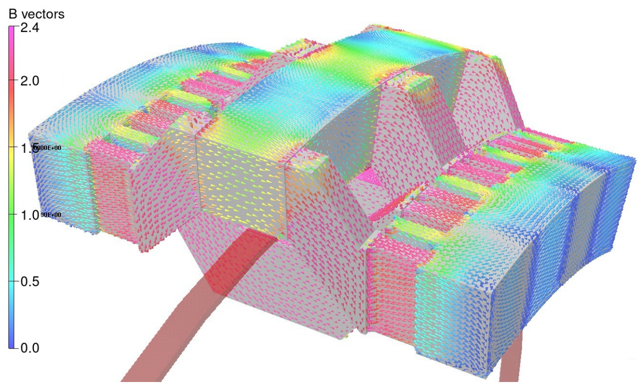

(c) Flux density vectors.

Figure 3: The double-claw pole machine model and flux density vectors.

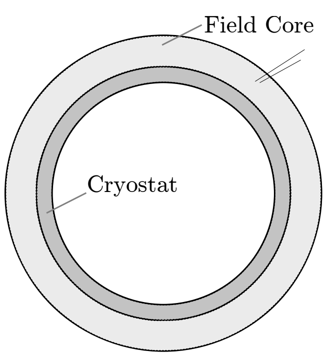

(a) Single cryostat.

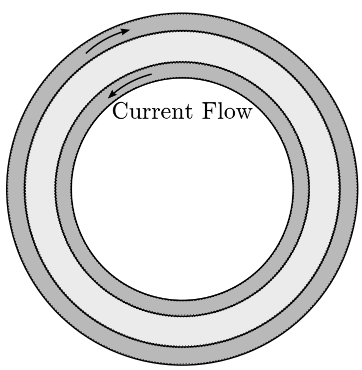

(b) Double cryostat.

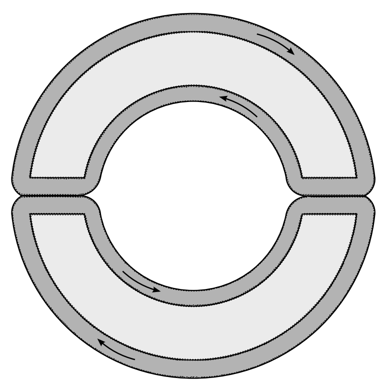

(c) Sectioned cryostats.

Figure 4: Sectioned cryostat design for the double-claw pole machine.

of the cryostats fails the machine can still operate at half-capacity until maintenance.

Power Rating	10 MW
Rotational Speed	10 rpm
Number of Poles	88
Outer Diameter	6.63 m
Armature Diameter	5.84 m
Rotor Radius	3.20 m
Inner Radius	2.29 m
Axial Length	1.38 m
Number of Stator Slots	66
Number of Turns	96
Induced Coil Voltage	173 V_{rms}
Phase Voltage Voltage	3.3 kV_{ll}

Table 2: Main specifications of the optimized 10 MW, 10 rpm design.

3. Design of a 10 MW Superconducting Generator

As presented in the introduction section and in Table 1, 10 MW, 10 rpm superconducting generator designs are quite common in the literature, therefore, a 10 MW double-sided claw pole machine is designed for a better comparison with other superconducting machine designs.

A parametrized FEA model of the proposed topology is developed, which estimates the air gap flux density and power output. The machine is optimized using the genetic algorithm optimization tool “rgenoud” [**?**]. The objective function is defined as the total active material mass, with pre-defined constraints in outer diameter, phase voltage and current density.

The main specifications of the optimum design is presented in 2 and the outline is shown in 5. The machine has an outer diameter of 6.6 m and an axial length of 1.4 m, which is a similar size to a 5 MW direct-drive permanent magnet generator. The machine has an electrical frequency of 7.33 Hz. There are 11 coils in series and two parallel branches for each phase.

Figure 6 shows the flux density distribution in the stator tooth when the large claw pole and small claw pole are aligned with the middle stator tooth. Mass estimations of the components are presented in Table **??**. The active material mass in the rotor is about 24 tonnes. Stators on each side weight around 10 tonnes.

3.1. Estimation of Losses

Main losses in the machine are presented in 4. Copper armature winding dissipates 510 kW of heat loss, which is cooled down by 40 kW of air blowers. Core losses in the machine are quite low due to an electrical frequency of 7.3 Hz.

It is important to accurately estimate the heat leakage in the cryostats, which

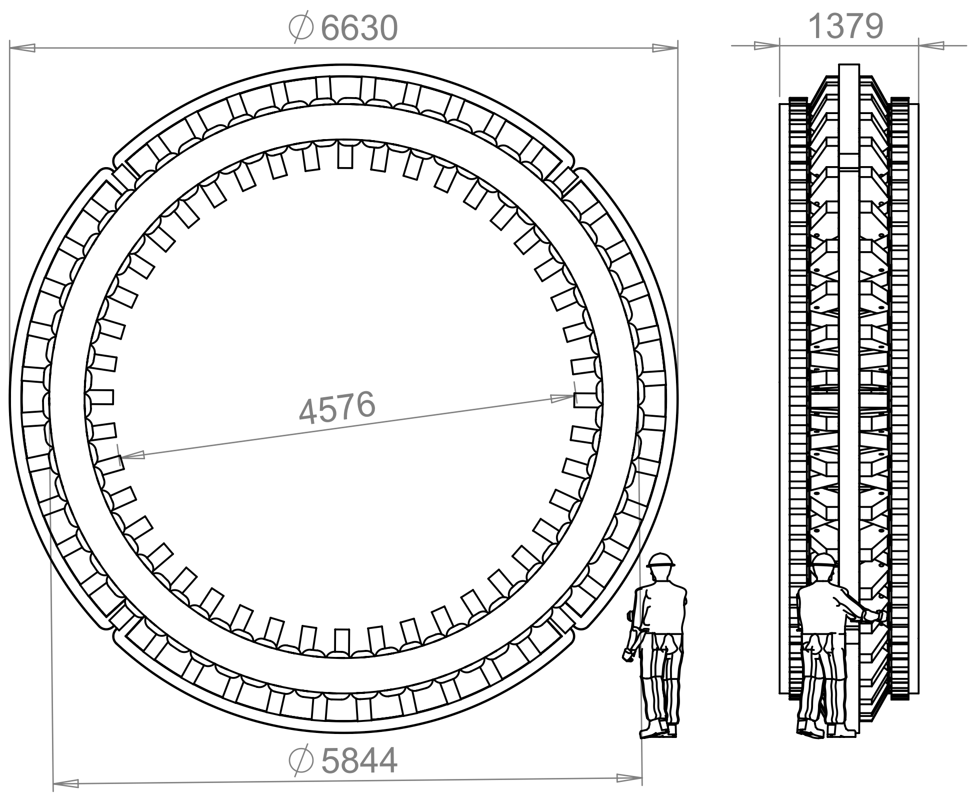

Figure 5: The outline dimensions of the 10 MW, 10 rpm generator design. Dimensions are in mm.

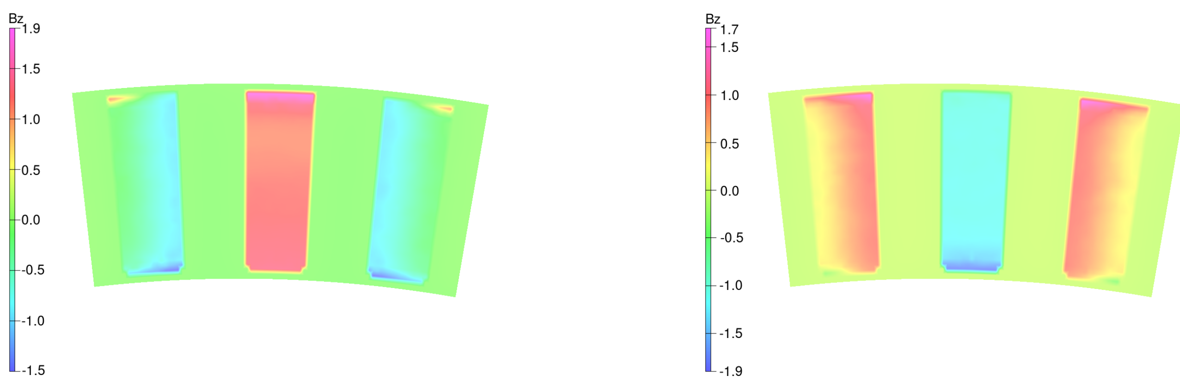

(a) Middle tooth aligned with the large claw pole.

(b) Middle tooth aligned with the small claw pole.

Figure 6: Flux density distribution in Z direction (into the page) in the stator teeth at mean coil radius.

Small Claw Pole	114 kg
Large Claw Pole	314 kg
Single Coil	17.5 kg
Stator Core (Single Side)	8,600 kg
Single Field Core Mass	2,830 kg
Cryostat Mass	1,200 kg
Cooling System Mass	2,000 kg
Total Rotor Active Material	23,850 kg
Stator (Single Side)	9,755 kg
Total Field Core Mass	11,320 kg
Total Active Material Mass	57,9 tonnes

Table 3: Mass estimations of the 10 MW, 10 rpm machine components.

Copper Loss	510 kW
Core Loss	7 kW
Cryocoolers	24 kW
Air Blowers (Armature)	40 kW
Efficiency	94.5 %

Table 4: Main losses and efficiency estimation for the 10 MW, 10 rpm design.

can be divided into gas heat conduction through the vacuum, radiation heat from warm walls of the cryostat, conduction through superconducting coil mechanical support, heat leakage through current leads and eddy current loss. These losses are estimated using the methodology presented in [**?**, **?**].

The surface area of a single cryostat is 6.1 m^2, which gives the total cryostat wall area as 24.4 m^2. The cryostat used in the proposed generator is different to a superconducting rotor, where a cylindrical cryostat is used. Assuming a 5 m diameter, surface area of a cylindrical cryostat can be calculated as 55 m^2, which is twice the area of the proposed cryostat. Thus, the heat loss through cryostat wall is lower.

The heat loss can be calculated as shown in [**?**]. The operating pressure is chosen as 10^{-3} Pa, which can be achieved using standard industrial equipments. The heat loss at this vacuum level is 3.9 W. Radiation loss is calculated as 17.5 W by using 10 mm of MLI insulation, which has 30 layers.

Suspension straps are required to mechanically support the superconducting coil. As there are no electromagnetic torque acting on the superconducting coil, the design of these suspension straps relatively straightforward compared to the torque tubes of other types of superconducting machines. The distance between suspension straps is assumed as 1 m, which gives 10 straps per cryostat. Assuming the straps are made of G10-CR fibreglass, the conduction heat loss can be calculated as 13.5 W per cryostat.

The length of current leads should be carefully assessed as it depends on two factors:

	30 K MgB2–90 A	65 K YBCO–120 A
Gas Conduction (at 10^{-3} Pa)	3.9 W	3.4 W
Suspension Straps	54.0 W	50.0 W
Radiation	17.5 W	17.4 W
Current leads	47.2 W	48.8 W
Cold-head sleeve	15.6 W	15.6 W
Eddy Current	4.0 W	4.0 W
Other	15.0 W	15.0 W
Total loss	157.2 W	154.2 W

Table 5: Thermal budget for the 10 MW, 10 rpm design.

resistive losses and heat conduction through ambient. For minimum losses, the resistive and conductive losses should be equal as presented in [?]. Assuming a current input of 90 A, the heat loss in a single current lead is found as 5.9 W (11.8 W per cryostat).

Total heat losses in the cryostats are tabulated in Table 5. The heat loss at 65 K is also presented, which is estimated as 154.2 W. The total thermal budget of the machine at 30 K is 157.2 W, slightly larger than the heat loss at 65 K. Adding 25% safety margin, the machine can be cooled using 4 x 50 W cryocoolers. A suitable cooling system for such a requirement is selected as Cryomech's Gifford-McMahon AL230 cold-head coupled with CP950 compressor, which can supply 60 W of cooling power at 30 K [?]. Total cooling system mass in the generator is calculated as 2,000 kg with an electrical power input of 24 kW.

To summarize, the proposed topology has the advantage of independent cryostats, which increases the modularity and overall availability of the system. The total cryostat wall area is smaller compared to the conventional cylindrical cryostats, which helps to reduce the gas conduction and radiation losses. However, the sectioned cryostat results in higher number of current leads and suspension straps which increases the conduction losses. In general, the heat loss is within the reasonable values. For example in [?], it is stated that six to ten CTI-1020 cryogenic coolers are used for AMSC's 10 MW superconducting generator, provides 280–450 W of cooling power. In [?], the total cooling requirement for the GE's 10 MW LTS superconducting generator is estimated as 131 W, and in [?], 500 W is defined as the upper limit of the cooling power for a 5 MW superconducting generator.

3.2. Superconducting Coil Requirements

The magneto-motive-force of the superconducting coil is selected by the optimisation algorithm as 32.4 kAt, which saturates the claw poles up to 2.3 T. Total superconducting coil requirement in four cryostats (4 x 10.4 m) can be calculated as 1348 kAt.m as shown in Table 6.

Mean turn length	10.4 m
MMF of the SC	32.4 kAt
Number of Cryostats	4
Total SC requirement	1348 kAt.m

Table 6: Superconducting winding specifications for the 10 MW, 10 rpm design.

	MgB2	YBCO	
Operating Temperature	30 K	30 K	65 K
Current ($0.8I_c$)	90 A	400 A	100 A
Number of turns	360	81	324
Wire thickness	0.67 mm	0.22 mm	0.22 mm
Wire width	3.65 mm	4.8 mm	4.8 mm
Wire length(per cryostat)	3744 m	842 m	3370 m
Wire length (total)	15.0 km	3.4 km	13.5 km

Table 7: Superconducting tape requirements for the 10 MW, 10 rpm design (MMF=32.4 kAt).

The required superconducting wire length is calculated for three cases: MgB2 at 30 K, YBCO at 30 K, YBCO at 65 K. In critical current calculations magnetic flux penetrating into the superconducting coil is taken into account. The results presented in Table 7 whow the SC wire requirement is substantially less than other superconducting designs. In Table 8, SC wire requirements of several 10 MW designs are compared. In particular, air-cored topologies require hundreds of kilometres of superconducting wire. The closest design is the AMSC [?], which requires 36 km of YBCO at 30 K. However, the proposed design just requires 3.4 km of YBCO at that temperature, which is less than one tenth of the AMSC's design.

The low SC requirement is due to two main reasons. Firstly, the coil is loop shaped, which results in better utilization of the MMF per length of the coil. Secondly, as shown in Figure 7, the magnetic gap in the claw pole topology equals to the mechanical gap. However, in a typical superconducting machine the flux has to pass through many layers (vacuum, radiation shield, EM shield, etc.) through the cryostat, which results in a much larger magnetic gap and increased MMF requirement.

To summarize, the proposed topology has the advantage of independent cryostats, which increases the modularity and overall reliability of the system. The total cryostat wall area is smaller compared to the conventional cylindrical cryostats, which helps to reduce the gas conduction and radiation losses. However, the sectioned cryostat results in higher number of current leads and suspension straps which increases the conduction losses. In general, the heat loss is within the reasonable values. For example in [?], it is stated that 6–10 CTI-1020 cryogenics are used for AMSC's 10 MW superconducting generator, which gives 280–450 W of cooling power. In [?], the total cooling requirement

Table 8: Comparison of superconducting wire requirements and total mass of 10 MW direct-drive superconducting generators.

	SC Wire Requirement	Total Mass
	15 km MgB2 (30 K)	
Proposed Design	3.4 km YBCO (30 K)	184 t
	13.5 km YBCO (65 K)	
Abrahamsen et. al. [?]	200–300 km YBCO	88 t
General Electric [?]	720 km NbTi	143 t
AMSC/Snitchler et. al. [?]	36 km YBCO (30K)	150 t
Sung et. al. [?]	586 km YBCO	147 t
Sung et. al. [?]	222 km Bi2223	196 t
Terao et. al. [?]	270 km HTS + 275 km MgB2	-
Kim et. al. [?]	919 km HTS	-
Quddes et. al. [?]	1050–1400 km HTS	-

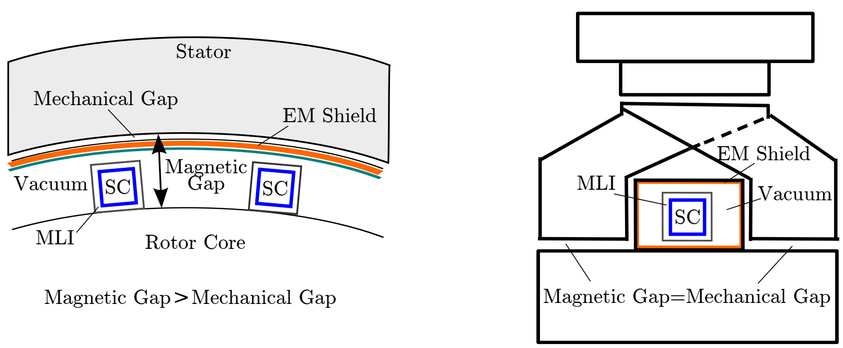

(a) Synchronous machine with superconducting rotor.

(b) Claw pole superconducting machine.

Figure 7: Magnetic and mechanical gap comparison for the typical superconducting machine and the claw pole machine.

for the GE's 10 MW LTS superconducting generator is estimated as 131 W. In [?], 500 W is defined as the upper limit of the cooling power for a 5 MW superconducting generator.

3.3. Structural Mass

The excess structural mass in the large direct-drive generators is a serious issue. A very stiff structure is required to keep the air-gap clearance and the structural mass increases significantly with diameter (the mass of the torque arms is proportional to R^3 [?]). The proposed machine has a smaller diameter than equivalent DDPM generators, which helps to reduce the structural mass. However, the high air-gap flux density increases the stress on the mechanical structure.

There are some studies trying to estimate the structural mass for DDPM generators

Power	Speed	Torque	Air-gap Diameter	Structural Mass
2 MW	19.5 rpm	979 kNm	4.3 m	14.6 t
3 MW	16 rpm	1790 kNm	5.1 m	19.6 t
5 MW	12.5 rpm	3820 kNm	6.1 m	50.1 t

Table 9: Structural mass estimation for different DDPM generators [?].

[?, ?]. In [?], the structural mass of different DDPM generators are compared (see 9). In [?] it is stated that the structural mass is around 55 % of the mass of a 5 MW DDPM generator. In [?], the structural mass of a 10 MW DDPM generator with 7 m air-gap diameter is estimated as 248 tonnes.

There are only a few studies that consider the structural mass in a superconducting machine design. In [?], the mass of superconducting and permanent magnet machines are compared. In [?], the structural mass of a 10 MW, 10 rpm superconducting generator is estimated as 76 tonnes for a YBCO wire based generator, and 102 tonnes for a Bi-2223 wire based generator. The structural mass for these machines are around 50 % of the overall mass.

Before proceeding into the structural mass estimation, it is useful to mention the different options to install the generator to the wind turbine nacelle. Firstly, an axial armature winding configuration with an inner rotor can be used as depicted in 8. In this configuration, the rotor structure is directly fixed to the turbine hub. The stator structure supports both of the armature windings. The forces acting on the claw poles are balanced, however there is a net magnetic attraction force on each armature core, and the stator structure should be stiff enough to cope with these forces. An alternative to eliminate these axial forces is to rotate the claw poles as shown in 9. In this configuration, the forces on the armature core act radially and cancel each other along the circular symmetry. The disadvantage of this symmetry is that the stators are no longer identical (i.e. the inner stator has a smaller diameter, which causes flux density and the induced voltage characteristics to differ). Although, the machine can be designed to minimise this effect, this configuration is not covered in this study and an axial armature configuration is assumed.

In [?], the structural mass for different types of DDPM generators are optimised. Zavvos used FEA simulations and analytical models to estimate the deflection in the structure due to tangential and normal stresses. An analytical model is presented to estimate the structural mass of machines depending on the diameter, axial length and air-gap flux density. Although, the topology is quite different, the analytical model for transverse flux permanent magnet generators presented in [?] is used to estimate the structural mass of the machine. The number of torque arms for stator and rotor is assumed to be 5, as it is found that it is the optimum value for minimum mass [?]. The mass of the rotor structure and stator structure is presented along with the active material mass in 10. Thus, the total mass of the generator is estimated as 184.2 t.

Rotor Structure	42.8 t
Stator Structure	83.5 t
Magnetic Core	52.4 t
Copper	2.3 t
Cooling - Cryostats	3.2 t
Total Mass	184.2 t

Table 10: The structural and active material mass estimations for the 10 MW, 10 rpm machine.

4. Mass Comparison

It is now time to revisit 1 of Chapter 1, which compares the torque densities of direct-drive permanent machines and superconducting machines. The 10 MW and 36.5 MW double-claw machine designs are placed in this graph in **??**. The mass of the double-claw machines are above the trend-line of the superconducting machines (by 23 % for the 10 MW machine, by the 36 % for 36.5 MW machine).

The subcomponents masses (structure, magnetic core, copper and cooling) are also presented in the figure. The structural mass dominates the total mass in both designs (68 % of the 10 MW design, 74 % of the 36.5 MW design). The magnetic core employs 28 % of the 10 MW design and 22 % of the 36.5 MW design. The magnetic core mass could be reduced in air-cored type superconducting generators, but the structural mass would still be significant due to high magnetic attraction forces in the machine.

5. Conclusions

In this chapter, a novel superconducting machine topology was presented, which is a modified version of the radial claw-pole design. In this concept, the forces acting on the rotor are balanced, so it is easier to manufacture the machine at large diameters. There is no need for SMC material as all the magnetic core sections can be manufactured from electrical steel laminations. Furthermore, the amount of the field core mass is reduced, which results in a lighter design.

A major advantage of the double-claw pole topology is its modularity; instead of using a single large circular superconducting coil, it can be divided into smaller sections. The armature winding also has similar modularity due to concentrated coils. This has the following advantages:

- Easier to manufacture and transport the machine.
- Independent operation of the cryostat sections.
- In the event of a fault in the cooling system or armature, the rest of the machine can be operated at part-load until maintenance.
- Faulty components can be replaced in situ.

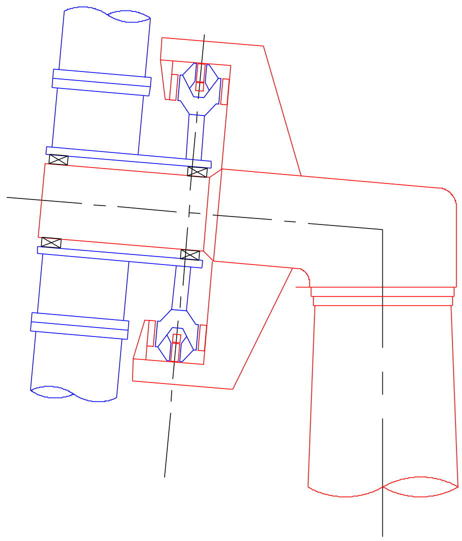

.4

Figure 8: Axial armature winding, inner rotor.

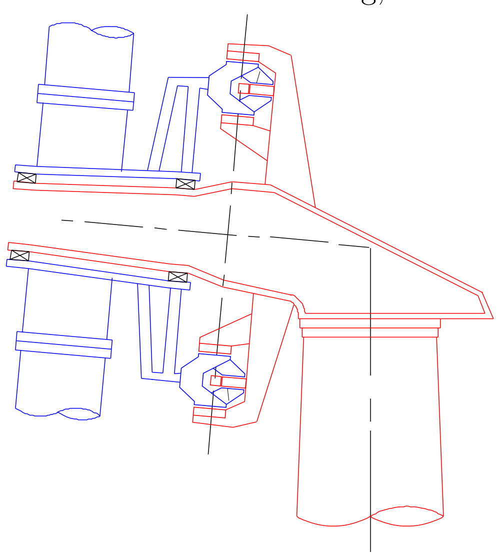

.4

Figure 9: Radial armature winding.

Figure 10: Two possible configurations for the installation of double-claw pole machine to a wind turbine (Drawings modified from [**?**]).

All these factors are very beneficial for offshore wind turbines, where the maintenance and installation are difficult and expensive.

In order to find the optimum design, a parametrized FEA model was developed and coupled with a genetic algorithm optimisation tool. The tool was used to design a 10 MW, 10 rpm generator for wind turbines and a 36.5 MW, 120 rpm machine as a ship propulsion motor.

The 10 MW machine has an outer diameter of 6.6 m and an axial length of 1.4 m. The active material mass of the machine was calculated as 58 tonnes. Including the structure and the cooling system, the total mass is estimated as 184 tonnes. This is 23 % higher than the trend-line of superconducting machines, but still 40 % lighter than the similar rated direct-drive permanent magnet generators. Structural mass is a significant component of total mass (around 70 %). In fact, it is expected that it will be similar for all superconducting machines due to high airgap flux densities, although, the structural mass is usually neglected in direct-drive superconducting machine designs. Further improvements can be made by developing novel structures, and coupling the optimisation with structural design.

One of the most important advantages of the proposed topology is the low superconducting wire requirement compared to other superconducting machine designs. For example, 10 MW air-cored superconducting generators require more than 500 km of superconducting wire (see **??**). Other machines require around 100 km of superconducting wire. However, the proposed 10 MW double-claw machine requires just 15 km MgB2 tape at 30 K or 13.5 km YBCO tape at 65 K. The electrical power required for cooling is estimated as 24 kW (just 0.24 % of the total power rating).

To conclude, it has been shown that, the claw pole topology can be applied as a direct-drive generator (and ship propulsion motor). In terms of mass, it may not be as competitive as other superconducting machine designs, but it has clear advantages in terms of modularity and increased reliability. Furthermore, it uses much less superconducting wire and is expected to be more cost-competitive than other superconducting generator designs.

References

[1] Goosens M, Rahtz S and Mittelbach F 1997 *The LaTeX Graphics Companion* (Reading, MA: Addison-Wesley)
[2] Reckdahl K 1997 *Using Imported Graphics in LaTeX* (search CTAN for the file 'epslatex.pdf')